Electronic Supplementary Material (ESI) for Dalton Transactions.
This journal is © The Royal Society of Chemistry 2021

Supplementary Information

Role of intramolecular hydrogen bonding in the redox chemistry of hydroxybenzoate-bridged paddlewheel diruthenium(II, II) complexes

Wataru Kosaka,[a,b] Yudai Watanabe,[b] Kinanti Hantiyana Aliyah,[b] and Hitoshi Miyasaka*[a,b]

[a] Institute for Materials Research, Tohoku University, 2-1-1 Katahira, Aoba-ku, Sendai 980-8577, Japan

[b] Department of Chemistry, Graduate School of Science, Tohoku University, 6-3 Aramaki-Aza-Aoba, Aoba-ku, Sendai 980-8578, Japan

Corresponding author*

Prof. Dr. Hitoshi Miyasaka

Institute for Materials Research, Tohoku University, 2–1–1 Katahira, Aoba-ku, Sendai, Miyagi 980-8577, Japan

E-mail: miyasaka@imr.tohoku.ac.jp

Tel: +81-22-215-2030

FAX: +81-22-215-2031

■ Contents for SI

Table S1. Crystallographic Data.

	***o*-OH**	***m*-OH**	**2,3-(OH)$_2$**	**2,4-(OH)$_2$**	**2,5-(OH)$_2$**	**2,6-(OH)$_2$**	**3,4-(OH)$_2$**
formula	$C_{40}H_{32}F_{12}O_{12}Ru_2$	$C_{48}H_{48}F_{12}O_{14}Ru_2$	$C_{40}H_{32}F_{12}O_{14}Ru_2$	$C_{48}H_{48}F_{12}O_{16}Ru_2$	$C_{48}H_{48}F_{12}O_{16}Ru_2$	$C_{40}H_{32}F_{12}O_{14}Ru_2$	$C_{56}H_{64}F_{12}O_{18}Ru_2$
formula weight	1134.81	1279.02	1166.79	1311.00	1311.00	1166.79	1455.21
crystal system	monoclinic	monoclinic	monoclinic	monoclinic	triclinic	triclinic	monoclinic
space group	$P2_1/n$	$P2_1/c$	$P2_1/c$	$P2_1/c$	$P\bar{1}$	$P\bar{1}$	$P2_1/n$
a / Å	10.9274(3)	12.7745(4)	11.5640(3)	13.7407(5)	9.2767(2)	9.5745(4)	18.1637(6)
b / Å	14.1299(2)	19.5988(4)	21.2804(5)	8.5407(3)	11.2427(2)	10.7072(4)	8.5969(3)
c / Å	14.5991(4)	10.8663(3)	9.1600(2)	22.0232(8)	25.2696(4)	10.8653(4)	20.5738(7)
α / deg	90	90	90	90	99.3040(10)	110.185(4)	90
β / deg	110.951(3)	112.948(3)	101.954(2)	100.872(3)	99.0110(10)	92.607(4)	111.700(4)
γ / deg	90	90	90	90	96.6480(10)	96.466(4)	90
V / Å^3	2105.12(10)	2505.23(13)	2205.27(9)	2538.15(16)	2541.67(8)	1034.55(7)	2984.96(19)
Z	2	2	2	2	2	1	2
crystal size / mm^3	0.17×0.14×0.09	0.18×0.12×0.05	0.21×0.12×0.03	0.15×0.12×0.02	0.32×0.22×0.10	0.38×0.10×0.03	0.26×0.16×0.01
T / K	103(1)	103(1)	93(1)	93(1)	93(1)	93(1)	93(1)
D_{calc} / g·cm^{-3}	1.923	1.695	1.757	1.715	1.713	1.873	1.619
F_{000}	1128.00	1288.00	1160.00	1320.00	1320.00	580.00	1480.00
λ / Å	0.71073	0.71073	0.71073	0.71073	0.71073	0.71073	0.71073
μ(Mo Kα) / cm^{-1}	8.330	7.130	8.010	7.090	7.080	8.540	6.140
data measured	13487	18663	17129	22890	20134	8630	23473
data unique	3770	5567	5018	5673	11151	4591	6840
R_{int}	0.0143	0.0269	0.0128	0.0258	0.0161	0.0333	0.0396
no. of observations	3770	5567	5018	5673	11151	4591	6840
no. of variables	298	343	328	354	707	309	271
$R1$ ($I > 2.00\sigma(I)$)[a]	0.0254	0.0262	0.0210	0.0284	0.0556	0.0330	0.0538
R (all reflections)[a]	0.0258	0.0285	0.0222	0.0344	0.0585	0.0364	0.0668
$wR2$ (all reflections)[b]	0.0663	0.0683	0.0541	0.0697	0.1267	0.0862	0.1375
GOF	1.125	1.053	1.055	1.049	1.042	1.058	1.132
CCDC No.	2121064	2121065	2121066	2121067	2121068	2121069	2121070

[a] $R1 = R = \Sigma||F_o|-|F_c||/\Sigma|F_o|$. [b] $wR2 = [\Sigma w(F_o^2-F_c^2)^2/\Sigma w(F_o^2)^2]^{1/2}$

Table S2. Magnetic parameters of $\{Ru_2^{II,II}((OH)_xPhCO_2)_2[2,6\text{-}(CF_3)_2PhCO_2]_2(THF)_2\}$ compounds obtained from the best-fit of χ vs. T data using a Curie equation for $S = 1$ with $g = 2.00$ (fix) and $zJ' = 0$ (fix).

Compound	D [K]	χ_{TIP} [$\times 10^{-6}$ cm^3 mol^{-1}]	ρ [$\times 10^{-3}$]
***o*-OH**	404.0(3)	49.1(14)	6.41(1)
***m*-OH**	357.4(6)	58(3)	40.7(2)
2,3-(OH)$_2$	389.0(9)	51(3)	41.2(5)
2,4-(OH)$_2$	370.3(9)	45(6)	25.4(2)
2,5-(OH)$_2$	374.3(5)	94(6)	5.069(9)
2,6-(OH)$_2$	406.8(9)	29(2)	83.9(6)
3,4-(OH)$_2$	368(3)	56(20)	67.9(7)

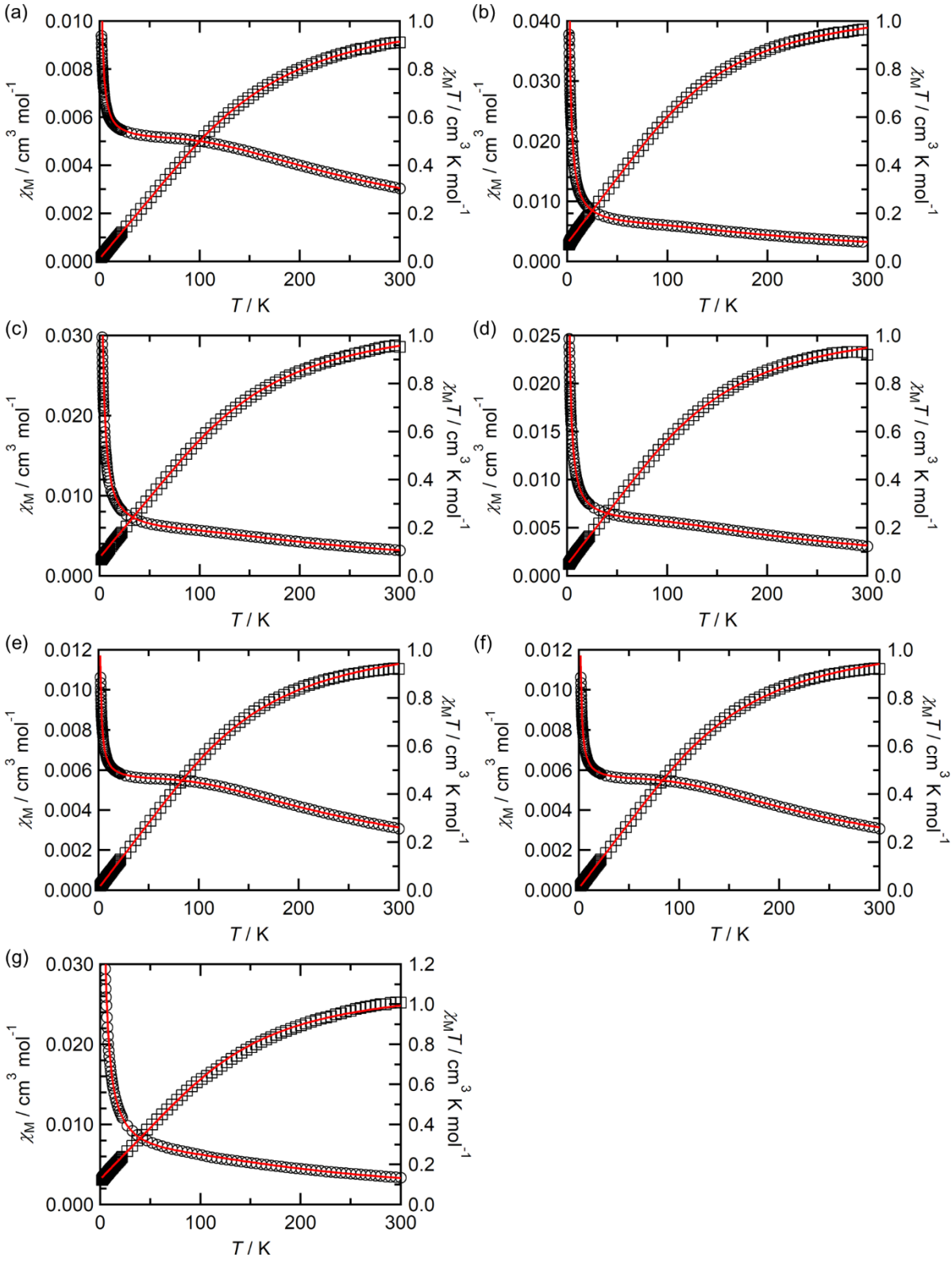

Fig. S1. Temperature dependence of χ (○) and χT (□) for ***o*-OH**, (a), ***m*-OH** (b), **2,3-(OH)$_2$** (c), **2,4-(OH)$_2$** (d), **2,5-(OH)$_2$** (e), **2,6-(OH)$_2$** (f), and **3,4-(OH)$_2$** (g), where the red solid lines represent simulated curves based on a Curie paramagnetic model with S = 1 taking into account zero-field splitting (D), temperature-independent paramagnetism (χ_{TIP}), and impurity with S = 3/2 (ρ).

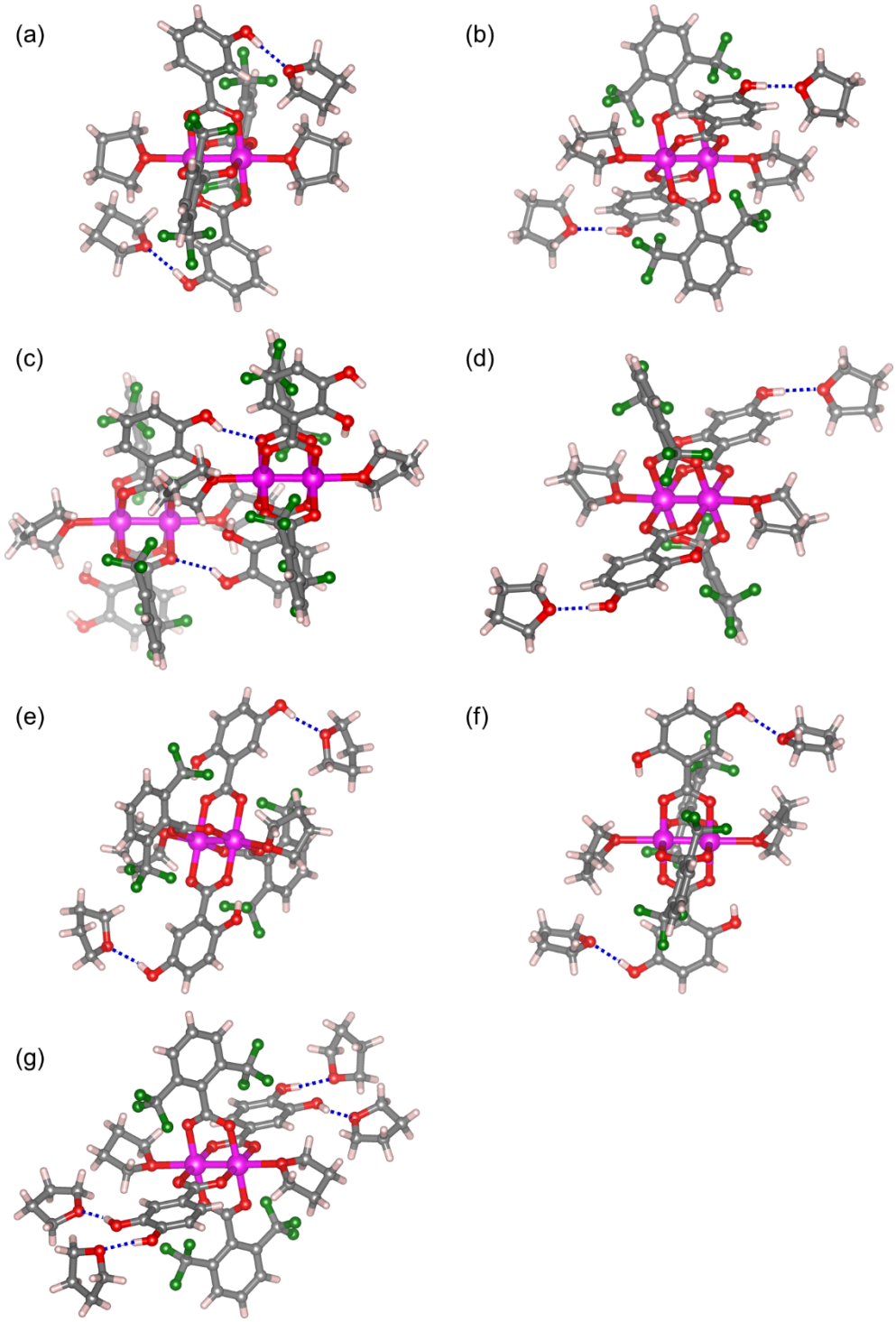

Fig. S2. Molecular structures focused on intermolecular hydrogen bond; ***m*-OH** (a), ***p*-OH** (b), **2,3-(OH)$_2$** (c), **2,4-(OH)$_2$** (d), **2,5-(OH)$_2$** (unit 1) (e), **2,5-(OH)$_2$** (unit 2) (f), and **3,4-(OH)$_2$** (g). Red, gray, green, light brown, and purple represent O, C, F, H, and Ru, respectively. Intermolecular hydrogen bond is depicted in blue dotted line.

Table S3. Estimated energy levels (eV) of π*- and δ*-characteristic orbitals for heteroleptic [$Ru_2^{II,II}$] complexes.

Electron character	**Orbital character**	***o*-OH**	***m*-OH**	***p*-OH**	**2,3-$(OH)_2$**	**2,4-$(OH)_2$**	**2,5-$(OH)_2$ Unit 1**	**2,5-$(OH)_2$ Unit 2**	**2,6-$(OH)_2$**	**3,4-$(OH)_2$**
β	π*	−2.03016	−1.85025	−1.76411	−2.10068	−2.02852	−2.10973	−1.99246	−2.27442	−1.82290
	π*	−2.10214	−1.91732	−1.81704	−2.19768	−2.09253	−2.27244	−2.14066	−2.37525	−1.87040
	δ*	−4.58993	−4.39969	−4.28771	−4.6716	−4.56404	−4.71222	−4.63712	−4.85384	−4.35035
α	δ*	−5.01294	−4.82229	−4.71104	−5.09395	−4.98743	−5.13418	−5.06134	−5.27588	−4.77383
	π*	−5.19623	−5.02057	−4.92953	−5.25951	−5.19147	−5.29438	−5.13925	−5.43116	−4.99432
	π*	−5.2867	−5.10610	−4.99616	−5.38148	−5.27495	−5.47512	−5.32988	−5.56303	−5.04974

Table S4. Estimated energy levels (eV) of π*- and δ*-characteristic orbitals of the heteroleptic [$Ru_2^{II,II}$] complexes obtained by DFT calculation for the hypothetical structural models without intra-molecular hydrogen bond.

Electron character	**Orbital character**	***o*-OH**	**2,3-$(OH)_2$**	**2,4-$(OH)_2$**	**2,5-$(OH)_2$ Unit 1**	**2,5-$(OH)_2$ Unit 2**	**2,6-$(OH)_2$**
β	π*	−1.55286	−1.55029	−1.58721	−1.60997	−1.51781	−1.34864
	π*	−1.58969	−1.60854	−1.60468	−1.81191	−1.67632	−1.37136
	δ*	−4.07649	−4.08802	−4.07787	−4.21542	−4.14782	−3.85097
α	δ*	−4.49935	−4.51079	−4.50124	−4.63691	−4.57198	−4.27336
	π*	−4.71551	−4.71382	−4.74478	−4.77797	−4.65971	−4.47866
	π*	−4.76044	−4.77244	−4.76895	−5.01527	−4.85819	−4.53299

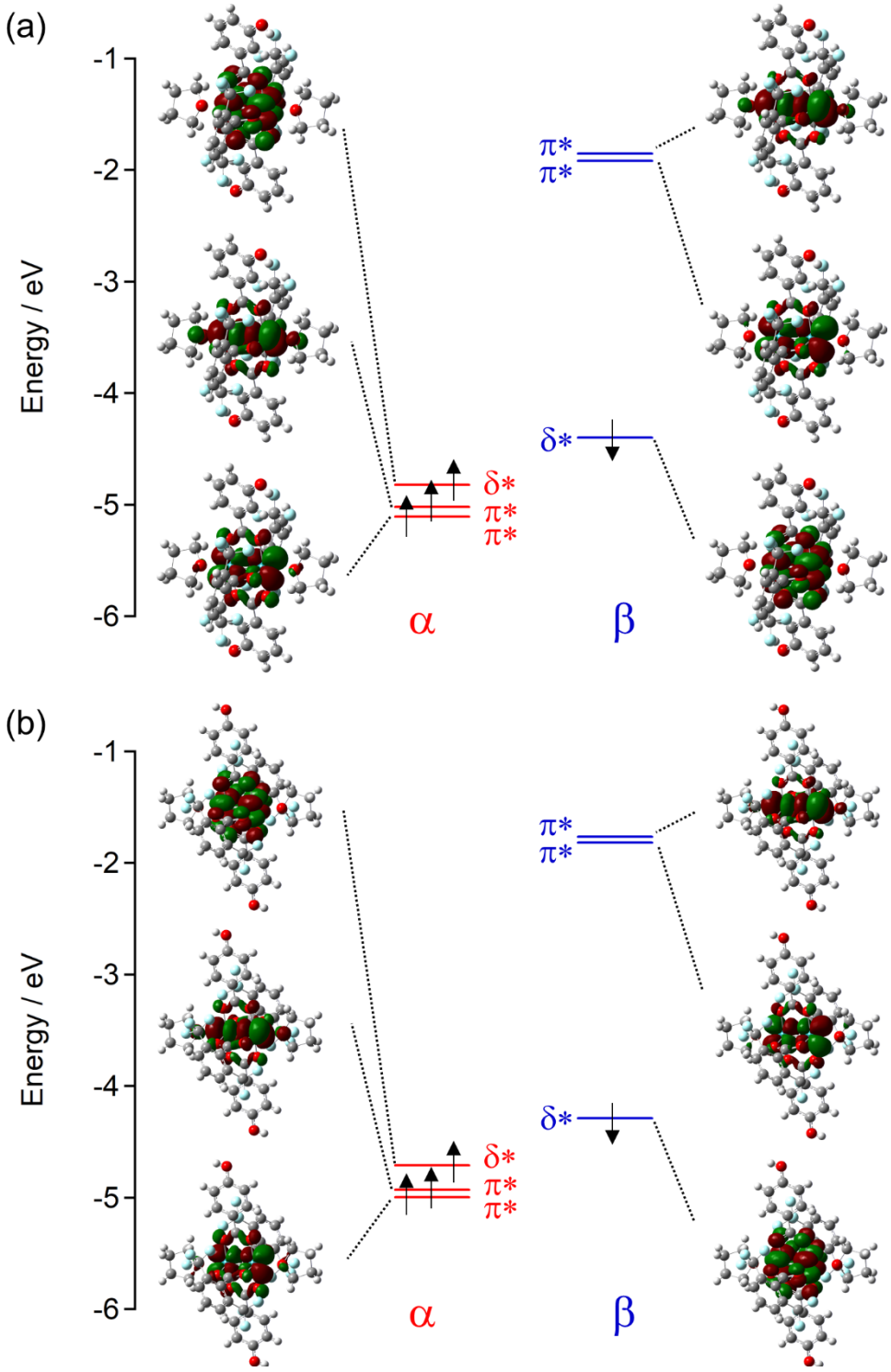

Fig. S3. Frontier orbitals associated with π* and δ* orbitals for ***m*-OH** (a) and ***p*-OH** (b), and their energy levels (eV), where δ* for b electron corresponds to HOMO level.

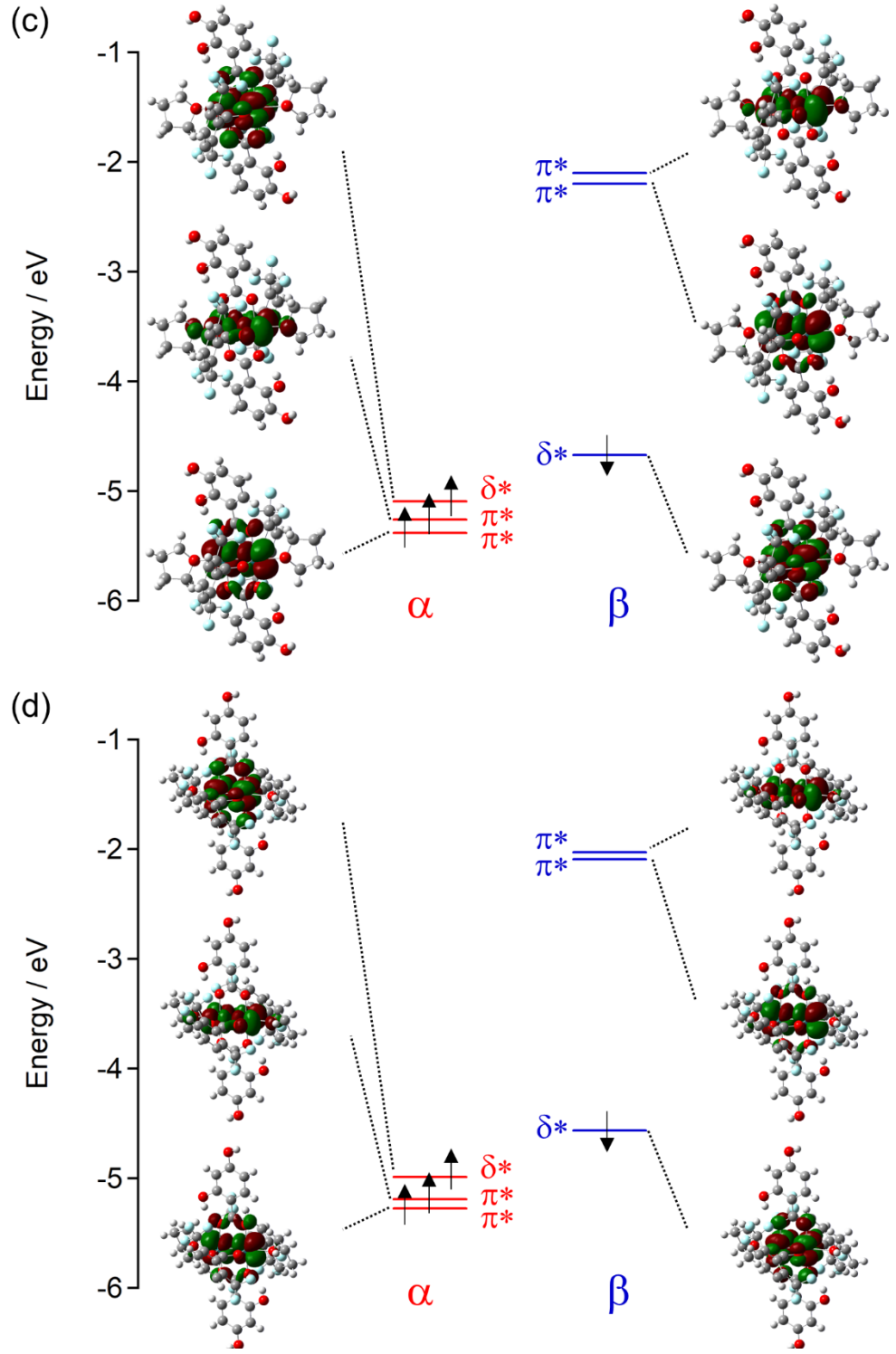

Fig. S3 (continued). Frontier orbitals associated with π* and δ* orbitals for **2,3-(OH)$_2$** (c) and **2,4-(OH)$_2$** (d), and their energy levels (eV), where δ* for b electron corresponds to HOMO level.

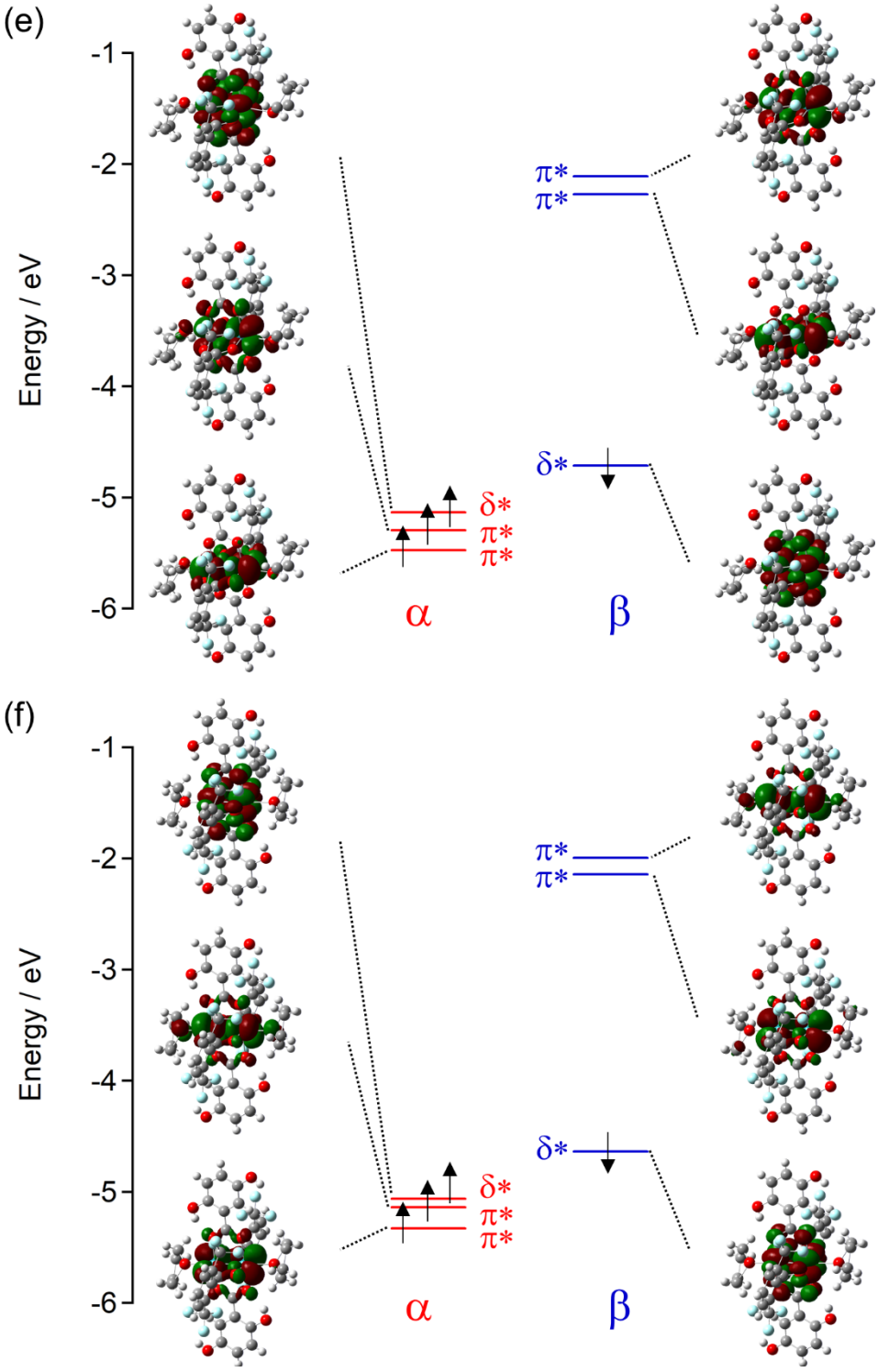

Fig. S3 (continued). Frontier orbitals associated with π* and δ* orbitals for **2,5-(OH)$_2$** (unit 1) (e) and **2,5-(OH)$_2$** (unit 2) (f), and their energy levels (eV), where δ* for b electron corresponds to HOMO level.

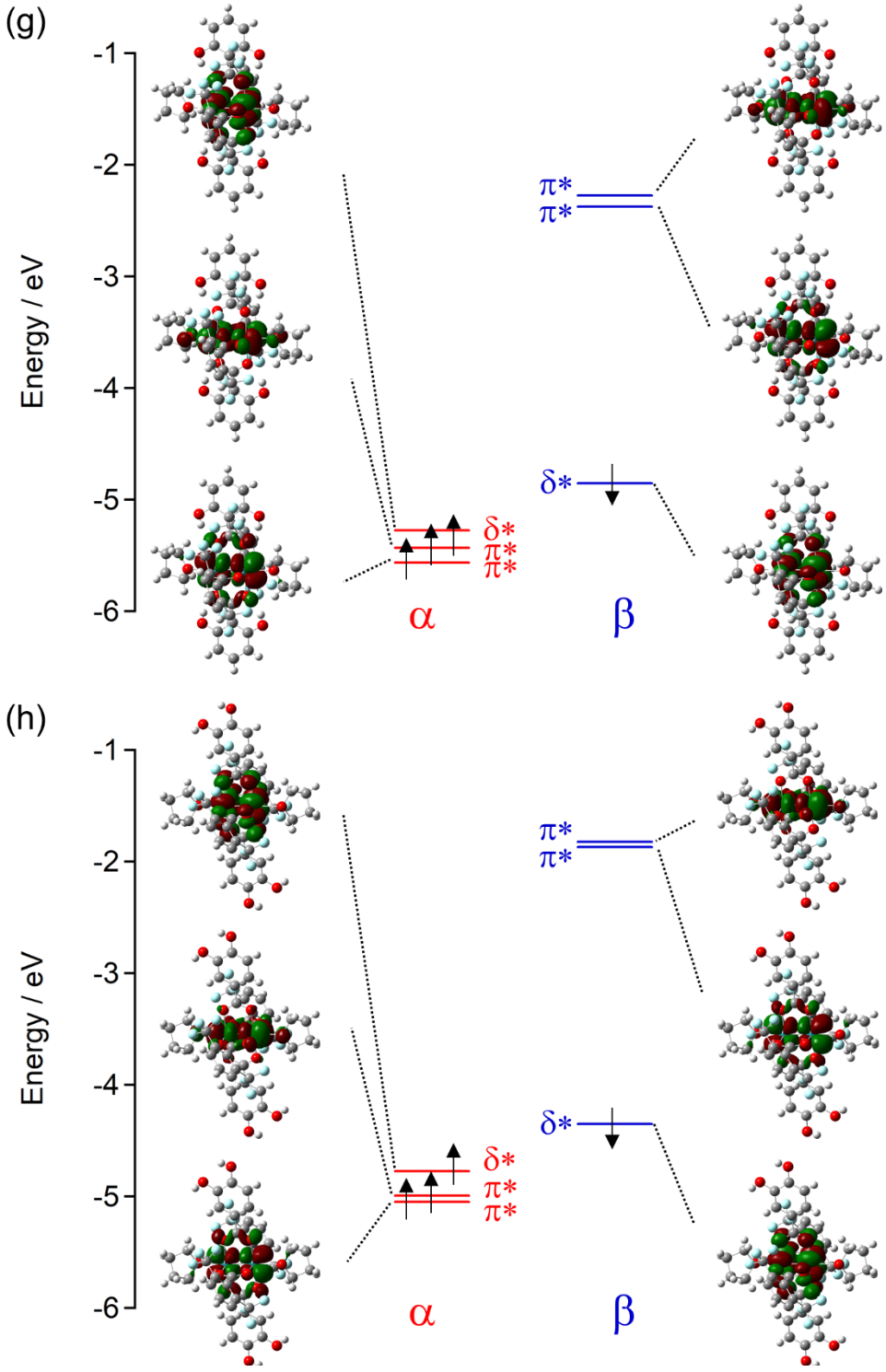

Fig. S3 (continued). Frontier orbitals associated with π* and δ* orbitals for **2,6-(OH)$_2$** (g) and **3,4-(OH)$_2$** (h), and their energy levels (eV), where δ* for b electron corresponds to HOMO level.

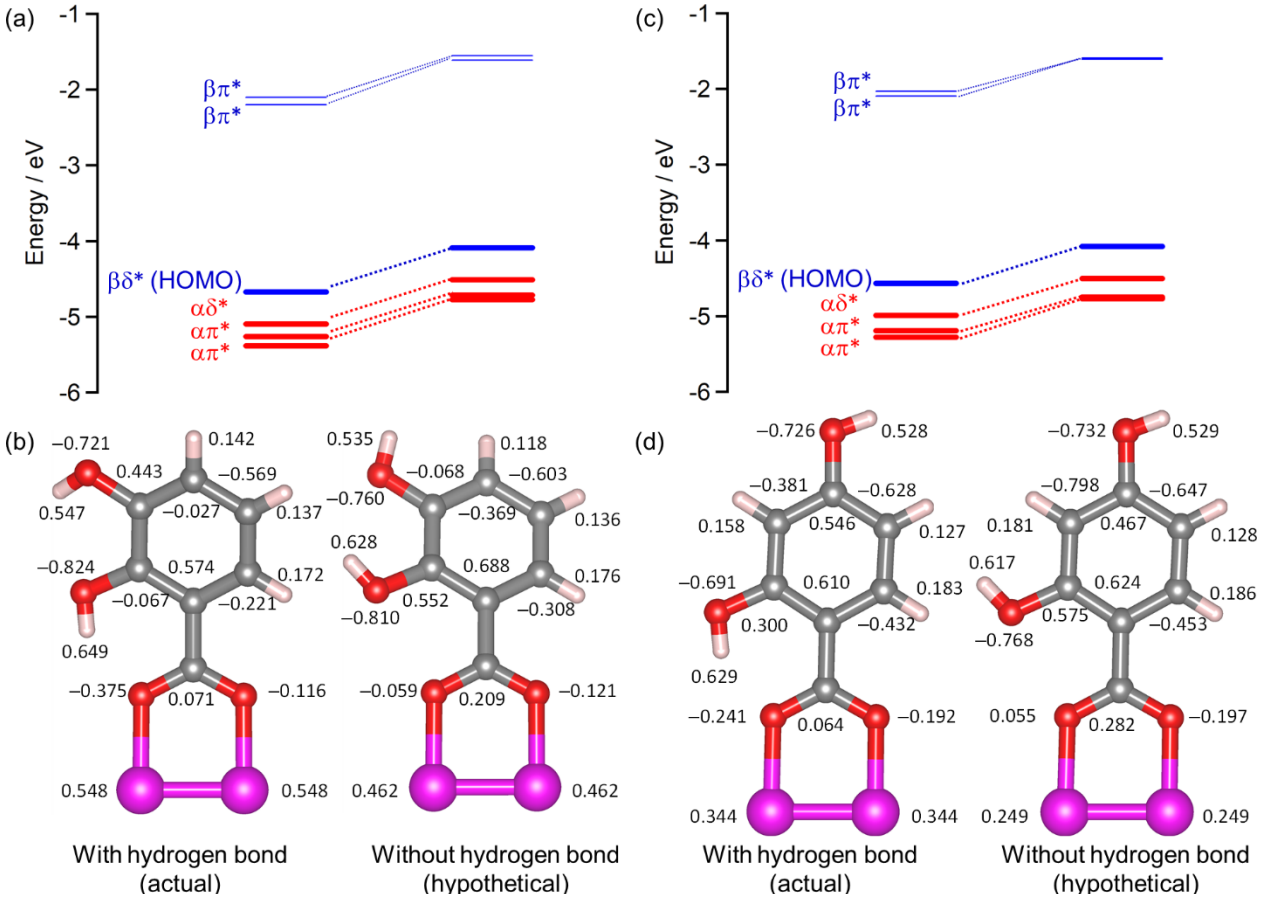

Fig. S4. Energy diagrams of frontier orbitals associated with π* and δ* orbitals for **2,3-(OH)$_2$** (a) and **2,4-(OH)$_2$** (c) obtained by DFT calculation for the structural models with (left) or without (right) intra-molecular hydrogen bond; a part of structural model of **2,3-(OH)$_2$** (b) and **2,4-(OH)$_2$** (d) subjected to DFT calculation; actual (left) or hypothetical (right) crystal structure with or without intra-molecular hydrogen bond, respectively. Attached digits indicate the value of Mulliken charge. Another bridging $(OH)_xPhCO_2^-$ and 2,6-$(CF_3)_2PhCO_2^-$ moieties, and THF molecules at axial position are omitted for clarity.

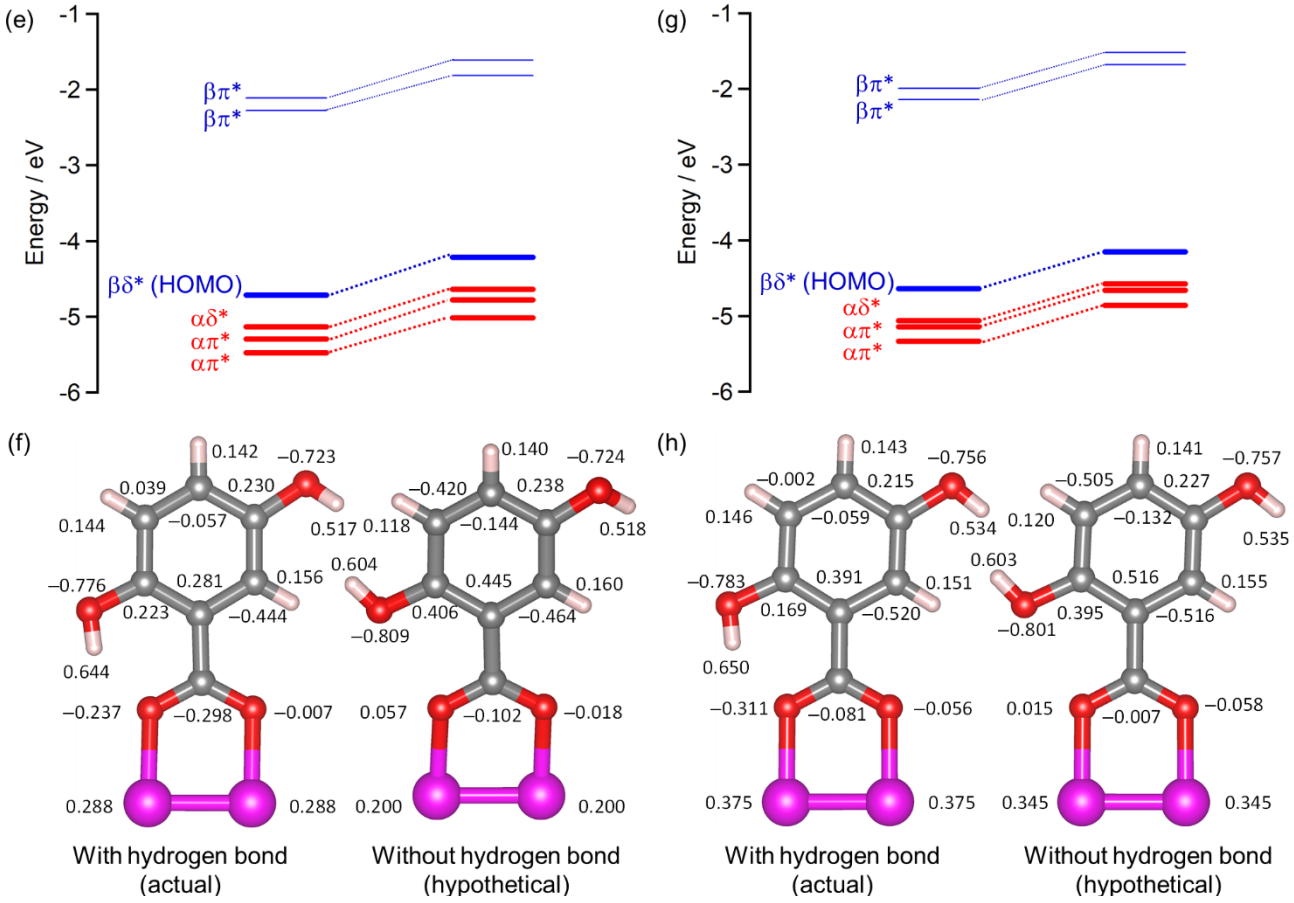

Fig. S4 (continued). Energy diagrams of frontier orbitals associated with π* and δ* orbitals for **2,5-(OH)$_2$** (unit 1) (e) and **2,5-(OH)$_2$** (unit 2) (g) obtained by DFT calculation for the structural models with (left) or without (right) intra-molecular hydrogen bond; a part of structural model of **2,5-(OH)$_2$** (unit 1) (f) and **2,5-(OH)$_2$** (unit 2) (g) subjected to DFT calculation; actual (left) or hypothetical (right) crystal structure with or without intra-molecular hydrogen bond, respectively. Attached digits indicate the value of Mulliken charge. Another bridging $(OH)_xPhCO_2^-$ and 2,6-$(CF_3)_2PhCO_2^-$ moieties, and THF molecules at axial position are omitted for clarity.

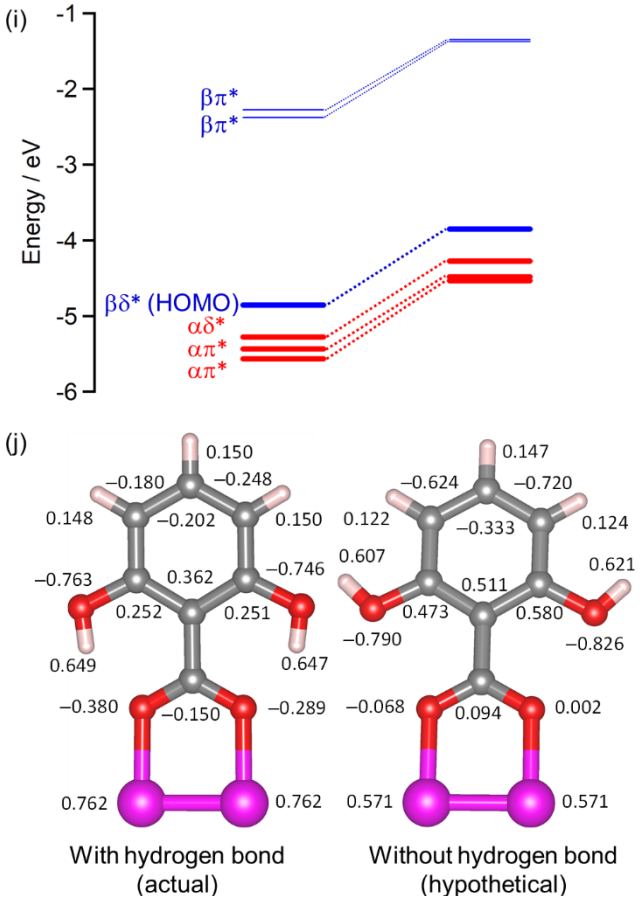

Fig. S4 (continued). Energy diagrams of frontier orbitals associated with π* and δ* orbitals for **2,6-(OH)$_2$** (i) obtained by DFT calculation for the structural models with (left) or without (right) intra-molecular hydrogen bond; a part of structural model of **2,6-(OH)$_2$** subjected to DFT calculation; actual (left) or hypothetical (right) crystal structure with or without intra-molecular hydrogen bond, respectively. Attached digits indicate the value of Mulliken charge. Another bridging $(OH)_xPhCO_2^-$ and 2,6-$(CF_3)_2PhCO_2^-$ moieties, and THF molecules at axial position are omitted for clarity.

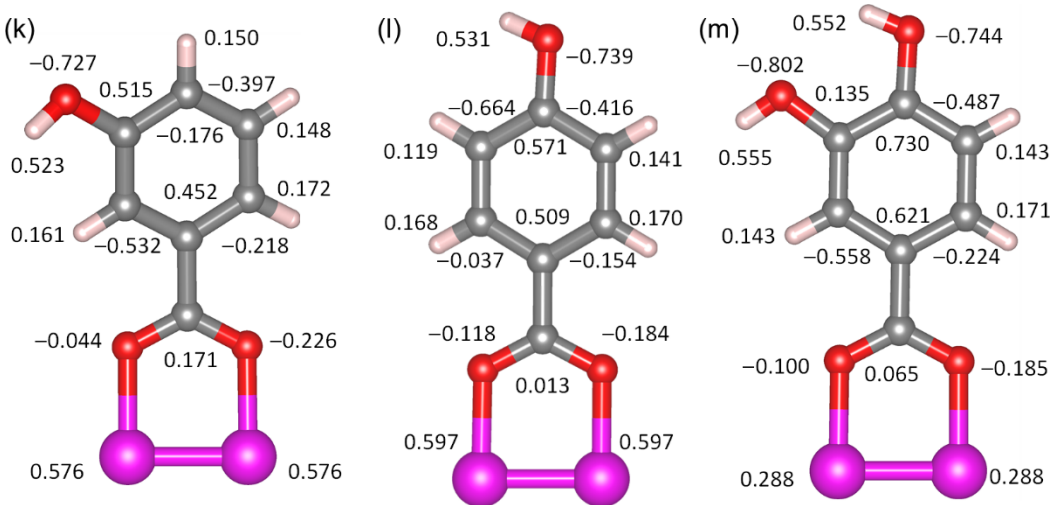

Fig. S4 (continued). A part of structural model of ***m*-OH** (k), ***p*-OH** (l), and **3,4-(OH)$_2$** (m) subjected to DFT calculation. Attached digits indicate the value of Mulliken charge. Another bridging $OH_xPhCO_2^-$ and 2,6-$(CF_3)_2PhCO_2^-$ moieties, and THF molecules at axial position are omitted for clarity.

Table S5. Difference of Mulliken charge on hydroxy-substituted benzoate between the model with or without intra-molecular hydrogen bond, where negative value indicates that the actual model with intra-molecular hydrogen bond is more negatively charged.

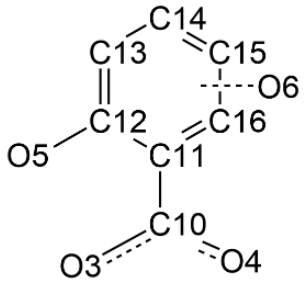

	***o*-OH**	**2,3-(OH)$_2$**	**2,4-(OH)$_2$**	**2,5-(OH)$_2$ Unit 1**	**2,5-(OH)$_2$ Unit 2**	**2,6-(OH)$_2$**
C10	−0.157	−0.138	−0.218	−0.196	−0.074	−0.244
C11	−0.167	−0.114	−0.014	−0.164	−0.125	−0.149
C12	−0.206	−0.619	−0.275	−0.183	−0.226	−0.221
C13	0.505	0.511	0.417	0.459	0.503	0.444
C14	0.067	0.342	0.079	0.087	0.073	0.131
C15	−0.009	0.034	0.019	−0.008	−0.012	0.472
C16	0.04	0.087	0.021	0.02	−0.004	−0.329
O3	−0.312	−0.316	−0.296	−0.294	−0.326	−0.312
O4	0.006	0.005	0.005	0.011	0.002	−0.291
O5	0.019	−0.014	0.077	0.033	0.018	0.027
O6	−−−	0.039	0.006	0.001	0.001	0.08
H5	0.038	0.021	0.012	0.04	0.047	0.042
H6	−−−	0.012	−0.023	0.026	0.026	0.026
H13	0.026	−−−	−0.001	0.002	0.002	0.003
H14	0.001	0.024	−−−	−0.001	−0.001	0.026
H15	0.000	0.001	−0.001	−−−	−−−	0.026
H16	−0.003	−0.004	−0.003	−0.004	−0.004	−−−
Total	**−0.152**	**−0.129**	**−0.195**	**−0.171**	**−0.100**	**−0.269**